

## Research Article

Haishui Han, Qun Zhang, Weifeng Lv, Lu Han, Zemin Ji, Shanyan Zhang, Changhong Zhao, Hao Kang\*, Linghui Sun and Rui Shen

# Experimental evaluation of velocity sensitivity for conglomerate reservoir rock in Karamay oil field

<https://doi.org/10.1515/secm-2022-0204>

received January 25, 2023; accepted April 24, 2023

**Abstract:** Velocity sensitivity refers to the possibility and degree of reservoir permeability decline caused by the migration of various particles in the reservoir rock due to the increase in fluid flow velocity and the blockage of pore channels. To improve the development results of M reservoir in Karamay Oil field, two reservoir cores were selected to carry out velocity sensitivity experiments. The permeability of No. 1 core decreases obviously when the flow rate is greater than 0.04 mL/min. Therefore, it can be considered that the injection rate of velocity sensitivity is between 0.04 and 0.06 mL/min, and the displacement rate should be less than 0.04 mL/min in the core displacement experiment. When the flow rate is greater than 0.5 mL/min, the permeability of No. 2 core decreases significantly. This is mainly due to the high permeability and critical velocity of No. 2 core. The study can provide a basis for the selection of displacement velocity in core displacement experiments, and also provide a reference for the determination of reasonable injection-production velocity in actual production.

**Keywords:** velocity sensitivity, formation sensitivity, core analysis, conglomerate reservoir, Karamay oil field

## 1 Introduction

The outbreak of the war between Russia and Ukraine has greatly affected the global security pattern and economic order. This impact has further brought challenges to the world's energy supply [1–4]. Many countries have experienced serious inflation, and the prices of oil and gas resources have been soaring, which has brought negative impacts on the healthy development of human society [5,6]. Therefore, for upstream oil and gas exploitation enterprises, how to maintain stable production and how to efficiently exploit underground oil and gas resources has always been a very meaningful topic. Meanwhile, with the development of the industrial era, lots of conventional oil and gas resources have been consumed, and oil and gas companies have to focus on unconventional oil and gas resources which are even more difficult to exploit [7–9]. Low permeable oil and gas reserves account for a considerable part of the global total oil and gas reserves, which still have great potential for development to meet the human demand. However, due to the uniqueness of the reservoir, the development of low permeable oil and gas also faces considerable difficulties [10–12]. In order to achieve efficient development of low permeable oil and gas fields, it is necessary to conduct comprehensive reservoir evaluation, so as to formulate reasonable development and adjustment schemes.

Velocity sensitivity damage of reservoir is the phenomenon of permeability reduction caused by the migration of clay mineral particles, which is an important factor affecting the normal production of crude oil. When the injection fluid carries solid particles into the well, if the size of the particles is smaller than the pore size of the formation, the particles will enter the formation and form a blockage near the small channel, resulting in a decrease in permeability. Additionally, if the injection fluid is incompatible with the original formation water, it will react with it to form sediment, and the sediment particles will be carried by the fluid to the small pore channel to form blockage. Therefore, it is of great significance to study

\* Corresponding author: Hao Kang, College of Engineering, Polytechnic Institute, Hebei Normal University, Shijiazhuang, China, e-mail: haokang@hebtu.edu.cn

Haishui Han, Qun Zhang, Weifeng Lv, Lu Han, Zemin Ji, Shanyan Zhang, Linghui Sun, Rui Shen: State Key Laboratory of Enhanced Oil Recovery, PetroChina, Beijing, China; Research Institute of Petroleum Exploration and Development, PetroChina, Beijing, China  
Changhong Zhao: Fengcheng Oilfield Operation Area of PetroChina, Xinjiang Oilfield Company, PetroChina, Karamay, China

the velocity sensitivity of reservoir for improving the oil recovery of oil field. Up to now, many scholars have carried out useful research on reservoir sensitivity evaluation.

In Guantao-Dongying Formation reservoir of Nanpu oil field, some production wells produce sand, and the pressure of water injection wells increases rapidly. Lu et al. [13] proved the existence of velocity sensitivity in the reservoir through the analysis of core velocity sensitivity experimental data. At the same time, the damage degree of velocity sensitivity of the reservoir is further revealed through the analysis of reservoir sensitivity minerals. The study is beneficial to control reasonable injection-production rate and enhance oil recovery. Wang et al. [14] compared and analyzed various prediction methods of reservoir sensitivity in recent years, and optimized a new method of coupling principal component analysis (PCA) and multiple nonlinear regression analysis. Taking salt sensitivity as an example, a mathematical model for predicting the damage index of salt sensitivity is established. With the demonstration of experimental data from Tarim oil field, the effectiveness and high accuracy of the algorithm of coupling PCA and multivariate nonlinear regression are proved. Sun et al. [15] considered that there should be two steps of drainage and gas production in the exploitation process of coalbed methane, and the existing evaluation method of core experiment by liquid flow cannot effectively evaluate its flow velocity sensitivity. Therefore, a new method of “gas-liquid equivalence” for flow velocity sensitivity evaluation is established, and a gas logging experimental method for flow velocity sensitivity of coalbed methane reservoir is established. The experimental results show that the gas logging method is suitable for the velocity sensitivity evaluation of coal reservoirs. Ao et al. [16] obtained the relationship between critical velocity and effective stress for the velocity sensitivity of fractured reservoir rock, considering the force on rock particles and different flow media, and combining with the regression of experimental curves. Finally, the critical production of producers and the critical injection volume of injectors are calculated by using the principle of fluid mechanics. This study is of good guiding significance for oil field production. Zhang et al. [17] used a new testing system to carry out an experimental study on the influence of pressure sensitivity of low permeability sandstone on production rate. Studies have shown that in the development of low permeability oil fields, it is beneficial to improve the ultimate recovery by reducing the bottom-hole flowing pressure step by step for many times and maintaining a reasonable production rate. Based on adequate study, Shi et al. [18] showed that the damage mechanism of reservoir velocity sensitivity is particle migration, and the

migratable particles include both clay mineral particles and non-clay mineral particles. The process of particle migration is analyzed from the perspective of mechanical theory, and it is pointed out that the critical velocity is a sign of velocity sensitivity damage. On the basis of laboratory experiments and mechanism studies, He et al. [19] improved the artificial neural BP network algorithm and compiled a software for predicting the five sensitivities of reservoirs. The field application results show that the software can provide reliable basis for the formulation of reservoir protection measures, thereby improving the efficiency of oil field development. Bai and Wang [20] used brine, kerosene, and refined oil as flowing media to study the damage degree of velocity sensitivity on reservoir rocks under different fluid viscosities, different cementation strengths, and different permeabilities. Yang et al. [21] calculated the velocity sensitivity damage radius and the optimal acidizing radius of the water injection wells based on the velocity sensitivity experiment and in combination with the field production parameters of the reservoir in Xing'anling Group through theoretical derivation. The field test confirmed that the design method has good practicability and can be used to guide the acidizing design of other sandstone reservoirs. Chen and Wang [22] used core flow experiment to study the influencing factors and injury degree of velocity sensitivity damage, which provided theoretical basis for reasonable operation system of producers and injectors. The results show that there are velocity-sensitive clay minerals in the reservoir of the target oil area and the degree of velocity-sensitive damage is weak to weak-neutral.

The geological reserves of low permeability reservoirs in Xinjiang oil field account for a relatively high proportion of the total reserves in the oil field, and some reservoirs show the characteristics of poor physical properties, low reserve abundance, and large range of burial depth. At the same time, there are many thin interbeds of sandstone and mudstone in the reservoir, and the microscopic characteristics and formation sensitivity are complex. With the deepening of the development process, the studies concerning reservoir sensitivity test experiments carried out for M reservoir are somewhat insufficient. Correspondingly, there is also a lack of systematic adjustment schemes to improve the development effect of the reservoir, which restricts its effective development. Through the experiment carried out in this research, it is beneficial to make up for the shortcomings of the research work of M reservoir by providing support for the references of low permeability reservoir sensitivity evaluation methods, the formation of low permeability reservoir differentiation development technology, and the formation of low permeability reservoir differentiation adjustment technology.

To be specific, the relative density of crude oil in M reservoir of Karamay oil field in Xinjiang is  $0.8588 \text{ g/cm}^3$ , and the viscosity of crude oil is  $27.11 \text{ mPa s}$  at  $50^\circ\text{C}$ , which belongs to medium viscosity crude oil. Clay minerals are mainly illite-montmorillonite mixed layer (montmorillonite), and the cementation between particles is loose, which makes it easy for particles to migrate and block the throat. Due to the strong velocity sensitivity of the reservoir, the permeability of the reservoir and the injection capacity of the injection well decrease in the process of water injection development, which seriously affects the development effect of the production well. In view of such production problems, it is necessary to carry out core velocity sensitivity evaluation. Through the research of this project, it aims to guide the oil field to further optimize the development plan, ensure the production, and provide a theoretical basis for the field development practice.

## 2 Experimental methods

Select two formation cores for velocity sensitivity test marked as No. 1 and No. 2, and the specific experimental method is conducted in accordance with China petroleum and natural gas industry standard SYT5358-2010 "Formation damage evaluation by flow test."

The rate of change of permeability due to flow rate sensitivity is calculated according to the following formula (1):

$$D_w = \frac{|K_w - K_i|}{K_i} \times 100\%, \quad (1)$$

where,  $D_w$  is the corresponding change rate of core permeability at different flow rates,  $K_w$  is the core permeability corresponding to different flow rates in the experiment,  $10^{-3} \mu\text{m}^2$ , and  $K_i$  is the initial permeability (core permeability corresponding to the minimum flow rate in the experiment),  $10^{-3} \mu\text{m}^2$ .

The experimental flow is converted into the seepage velocity according to the following formula (2):

$$v = \frac{14.4Q}{A \cdot \Phi}, \quad (2)$$

where,  $v$  is the fluid seepage velocity,  $\text{m/day}$ ;  $Q$  is the flow rate,  $\text{cm}^3/\text{min}$ ;  $A$  is the cross-sectional area of core,  $\text{cm}^2$ ; and  $\Phi$  is the porosity of core.

Velocity sensitive damage rate can be calculated according to formula (3):

$$D_v = \max(D_{v1}, D_{v2}, \dots, D_{vn}), \quad (3)$$

where,  $D_v$  is the velocity sensitive damage rate;  $D_{v1}$ ,  $D_{v2}$ , ...,  $D_{vn}$  are the permeability damage rates under different flow velocities.

The damage degree of velocity sensitivity is evaluated according to the following standards: when  $D_v \leq 5$ , the damage of fluid flow to reservoir permeability can be ignored. When  $5 < D_v \leq 30$ , the damage of fluid flow to reservoir permeability is weak. When  $30 < D_v \leq 50$ , the damage of fluid flow to reservoir permeability is moderate to weak. When  $50 < D_v \leq 70$ , the damage of fluid flow to reservoir permeability is moderate to strong. When  $D_v > 70$ , the damage of fluid flow to reservoir permeability is strong.

## 3 Experimental procedure

The length of core No. 1 is  $8.551 \text{ cm}$  with a core diameter of  $3.814 \text{ cm}$ , the gas-logging porosity is  $11.552\%$ , and the gas-logging permeability is  $1.610 \text{ mD}$ . Core No. 2 has a length of  $6.984 \text{ cm}$ , with a core diameter of  $3.818 \text{ cm}$ , a gas-logging porosity of  $10.073\%$ , and a gas-logging permeability of  $9.698 \text{ mD}$  (Figure 1).

In order to make the experimental results as accurate as possible, all the original fluids in the rock sample are cleaned. In consideration of the influence of the solvent and cleaning method in cleaning core pores on clay



Figure 1: Picture of natural conglomerate core.



minerals, the mixture of alcohol and benzene is used to clean the crude oil first, and then methanol is used to remove the salt.

Figure 2 shows the fracture of No.1 core after oil washing due to the loose cementation of the core. Adhesive 7102AB was selected for bonding and repairing to facilitate subsequent permeability and porosity measurements.

The conventional permeameter is used for test which is based on the steady state method. A certain pressure is applied to the inlet of the core sample. When the distribution of the gas pressure along the sample length is stable, the gas pressure at each point along the sample length only changes with the displacement and does not change with time, and then the permeability is calculated according to Darcy's formula. The steady state permeability meter can only be used for medium and high permeability samples, and it is not suitable for measuring

low permeability samples that do not obey Darcy's law. The PDP-200 permeability tester is suitable for measuring the permeability of conventional low and ultra-low permeability cores. The steady state method (pressure pulse attenuation method) is used for this testing, and the measurement time is short with high testing speed. The measurement process is automatic, and the opening and closing of important valves are automatically controlled by the computer. The computer automatically collects and records the data, and automatically calculates the permeability.

Key parameters of PDP permeability testing are as follows:

PDP permeability test range: 1–10 mD; porosity test range: 1.0–30.1%; core size: diameter 1–1.5"; length: 0–3"; and overburden pressure up to 10,000 psi. (Figures 3 and 4)

In order to ensure that the properties of clay in the core do not change, the drying temperature is controlled at 80°C, the relative humidity is controlled at 40–50%, the drying time is more than 48 h, and the difference between two consecutive weighing is less than 10 mg. Because the experimental core is dense conglomerate, the surface of the core is sealed with epoxy resin (the end face is left not sealed for experimental test) to prevent the core from breaking again.

In order to achieve the viscosity of crude oil under reservoir conditions, the degassed crude oil and kerosene were prepared for substitute of experimental oil according to the ratio of 1:1. Based on the experimental analysis, formation water ion composition is shown in Table 1. The ion equivalent of  $\text{CO}_3^{2-}$  is 178.52 mg/L, the ion equivalent of  $\text{HCO}_3^-$  is 1209.79 mg/L, the ion equivalent of  $\text{SO}_4^{2-}$  is 630.99 mg/L, the ion equivalent of  $\text{Cl}^-$  is 13507.20 mg/L, the ion equivalent of  $\text{Ca}^{2+}$  is 214.30 mg/L, the ion equivalent of  $\text{Mg}^{2+}$  is 39.13 mg/L, the ion equivalent of  $\text{Na}^+ + \text{K}^+$  is 9301.99 mg/L, the ion equivalent of total mineralization is 24075.75 mg/L, and the water type is  $\text{NaHCO}_3$  type.



Figure 2: Photos of core No. 1 after washing oil.



Figure 3: Pictures of PDP permeability tester, steady state permeability tester, and porosity tester.



Figure 4: Core samples after epoxy treatment.

Chemical composition of formation water is shown in Table 2. The ion equivalent of NaCl is 21.49 g/L, the ion equivalent of  $\text{NaHCO}_3$  is 1.67 g/L, the ion equivalent of  $\text{Na}_2\text{SO}_4$  is 0.93 g/L, the ion equivalent of  $\text{Na}_2\text{CO}_3$  is 0.32 g/L, the ion equivalent of  $\text{MgCl}_2 \cdot 6\text{H}_2\text{O}$  is 0.25 g/L, and the ion equivalent of anhydrous  $\text{CaCl}_2$  is 0.59 g/L.

Finally, the required content of various components is calculated according to  $\text{NaHCO}_3$  type formation water and prepared accordingly.

Ion composition of injected water is shown in Table 3. The ion equivalent of  $\text{CO}_3^{2-}$  is 537.76 mg/L, the ion equivalent of  $\text{HCO}_3^-$  is 756.34 mg/L, the ion equivalent of  $\text{SO}_4^{2-}$  is 73.16 mg/L, the ion equivalent of  $\text{Cl}^-$  is 6593.88 mg/L, the ion equivalent of  $\text{Ca}^{2+}$  is 170.15 mg/L, the ion equivalent of

$\text{Mg}^{2+}$  is 15.27 mg/L, the ion equivalent of  $\text{Na}^+ + \text{K}^+$  is 4785.94 mg/L, and the ion equivalent of total mineralization is 12932.5 mg/L.

Chemical composition of injected water is shown in Table 4. The ion equivalent of NaCl is 12.17 g/L, the ion equivalent of  $\text{NaHCO}_3$  is 1.04 g/L, the ion equivalent of  $\text{Na}_2\text{SO}_4$  is 0.11 g/L, the ion equivalent of  $\text{Na}_2\text{CO}_3$  is 0.95 g/L, the ion equivalent of  $\text{MgCl}_2 \cdot 6\text{H}_2\text{O}$  is 0.13 g/L, and the ion equivalent of anhydrous  $\text{CaCl}_2$  is 0.47 g/L.

HAAKE MARS III rheometer is used according to the China Petroleum and Natural Gas Industry Standard SY/T 7549-2000-Determination of Viscosity-Temperature Curve of Crude Oil-Rotational Viscometer Method, and the appropriate shear rate is selected to measure the viscosity-temperature curve of the experimental oil. The results are shown in Table 5 and Figure 5, respectively. The viscosity of the experimental oil is relatively low and has good fluidity at normal temperatures.

The results of various mineral components analysis, through the X-ray diffraction experiment, are shown in Tables 6 and 7.

It can be seen from Table 6 that the clay contents of samples 1 and 2 are relatively high, which are 29.6 and 13.2%, respectively. To be specific, as for core No. 1, the content of quartz is 17.6%, the content of potassium feldspar is 5.8%, the content of plagioclase is 38.1%, the content of calcite is 2.7%, the content of anhydrite is 2.1%, the content of ankerite is 2.3%, and the content of mica is 1.8%. For core No. 1, the content of ankerite is 2.3%, and the content of mica is 1.8%. For core No. 2, these two contents should be both zero.

Table 1: Formation water ion composition

Ion type	$\text{CO}_3^{2-}$	$\text{HCO}_3^-$	$\text{SO}_4^{2-}$	$\text{Cl}^-$	$\text{Ca}^{2+}$	$\text{Mg}^{2+}$	$\text{Na}^+ + \text{K}^+$	Total mineralization	Water type
Ion equivalent (mg/L)	178.52	1209.79	630.99	13507.20	214.30	39.13	9301.99	24075.75	$\text{NaHCO}_3$

Table 2: Chemical composition of formation water

Ion type	NaCl	$\text{NaHCO}_3$	$\text{Na}_2\text{SO}_4$	$\text{Na}_2\text{CO}_3$	$\text{MgCl}_2 \cdot 6\text{H}_2\text{O}$	Anhydrous $\text{CaCl}_2$
Ion equivalent (g/L)	21.49	1.67	0.93	0.32	0.25	0.59

Table 3: Ion composition of injected water

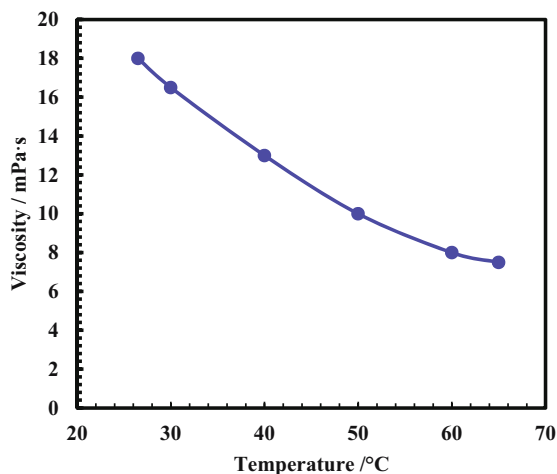
Ion type	$\text{CO}_3^{2-}$	$\text{HCO}_3^-$	$\text{SO}_4^{2-}$	$\text{Cl}^-$	$\text{Ca}^{2+}$	$\text{Mg}^{2+}$	$\text{Na}^+ + \text{K}^+$	Total mineralization	Water type
Ion equivalent (mg/L)	537.76	756.34	73.16	6593.88	170.15	15.27	4785.94	12932.5	$\text{NaHCO}_3$

**Table 4:** Chemical composition of injected water

Ion type	NaCl	NaHCO <sub>3</sub>	Na <sub>2</sub> SO <sub>4</sub>	Na <sub>2</sub> CO <sub>3</sub>	MgCl <sub>2</sub> ·6H <sub>2</sub> O	Anhydrous CaCl <sub>2</sub>
Ion equivalent (g/L)	12.17	1.04	0.11	0.95	0.13	0.47

**Table 5:** Viscosity–temperature data of experimental oil

Temperature (°C)	Speed (rpm)	Viscosity (mPa·s)
26.5	30	18.5
30	30	16.5
40	60	13
50	60	10
60	60	8
65	60	7.5

**Figure 5:** Viscosity–temperature curve of experimental oil.

It can be seen from Table 7 that the main clay minerals of core 1 contain a high content of illite-smectite mixed layer, accounting for 35%, and the mixed layer ratio is 58%; the main clay minerals of core 2 contain 19% of illite-smectite mixed layer, and the mixed layer ratio is 29%. Montmorillonite is the main mineral component of water sensitivity, and it will expand violently when it comes in contact with water, which will greatly reduce the permeability of core and the fluidity of fluid.

Take No.1 and No.2 cores for velocity sensitivity test, and dry No.2 core first, specifically, dry it at 105°C for 24 h, and then dry it at 80°C for 48 h for velocity sensitivity test.

In order to reduce the influence of core water sensitivity, two times of formation water and 2% of anti-swelling agent are used in the experiment. Use the displacement pump to adjust the injection rate to 0.01, 0.02, 0.04, 0.06, 0.08 mL/min, and so on, increasing the injection rate each time. Ensure that the injection volume is more than two pore volume (PV) at each injection rate, measure the displacement pressure after the pressure is stable, and calculate the liquid permeability. The displacement velocity–damage rate curve and the displacement velocity–permeability change curve are drawn, respectively, to observe the change in core permeability with the injection rate. The point where the permeability decreases significantly is the critical injection rate at which the velocity sensitivity occurs.

According to Stokes sedimentation theorem in fluid mechanics, clay mineral samples with particle size less than 10  $\mu\text{m}$  and less than 2  $\mu\text{m}$  were extracted by water suspension separation method or centrifugal separation method, respectively. Clay mineral samples with particle size less than 10  $\mu\text{m}$  were used to determine the total relative content of clay minerals in the original rock; clay mineral samples with particle size less than 2  $\mu\text{m}$  were used to determine the relative content of various clay minerals. The crystal of a mineral has a specific X-ray diffraction pattern, and the intensity of the characteristic peak in the pattern is positively correlated with the content of the mineral in the sample. The positive correlation K value between the content of a mineral and the intensity of its characteristic diffraction peak can be determined by means of experiments, and then the content of the mineral can be calculated by

**Table 6:** Results of X-ray diffraction analysis of mineral species

Core	Mineral type and content (%)							Total clay minerals (%)
	Quartz	Potassium feldspar	Plagioclase	Calcite	Anhydrite	Ankerite	Mica	
No. 1	17.6	5.8	38.1	2.7	2.1	2.3	1.8	29.6
No. 2	39.2	4.1	39.7	2.7	1.1	/	/	13.2

**Table 7:** Clay mineral type X-ray diffraction analysis result

Core	Relative content of clay minerals (%)						Mixed layer ratio, S, %	
	S	I/S	I	K	C	C/S	I/S	C/S
No. 1	/	35	40	11	14	/	58	/
No. 2	/	19	5	50	26	/	29	/

S: smectite; I/S: mixed layer of illite and smectite; I: illite; K: kaolinite; C: chlorite; C/S: mixed layer of chlorite and smectite.

measuring the intensity of the characteristic peak in an unknown sample.

## 4 Results and discussion

The displacement rate of No. 1 core increases from 0.01 mL/min, the displacement pressure increases gradually, the permeability measured by water decreases continuously, and the decreasing rate begins to increase at 0.04 mL/min until the displacement pressure increases to above 45 MPa after 0.08 mL/min, and the measurement cannot be continued due to the high pressure. The results are shown in Figure 6 and Table 8. Figure 6a shows the variation in  $D_{vn}$  with the change in displacement rate, and Figure 6b shows the variation in liquid permeability with the change in displacement rate.

The displacement rate of No. 2 core is increased from 0.01 to 1 mL/min, and the measurement is ended. With the increase in displacement rate, the permeability measured by water is gradually reduced, but it can be found that the reduction rate is significantly

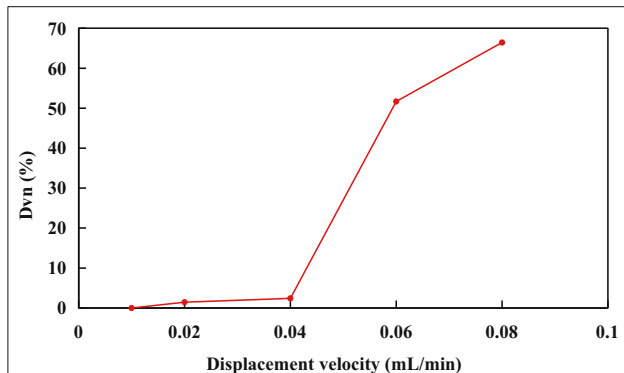
**Table 8:** Results of core velocity sensitivity test

Test results of core No. 1			
Injection velocity (mL/min)	Injection volume (PV)	Liquid permeability ( $10^{-3}$ mD)	$D_{vn}$ (%)
0.01	0.486	4.14	0.00
0.02	1.82	4.20	1.45
0.04	4.013	4.04	2.42
0.06	6.163	2.00	51.69
0.08	8.119	1.39	66.43

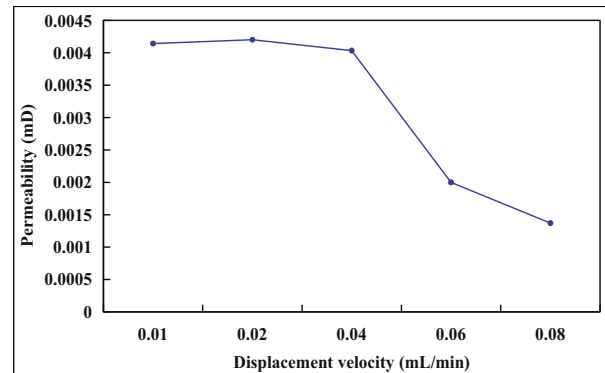
Test results of core No. 2			
Injection velocity (mL/min)	Injection volume (PV)	Liquid permeability (mD)	$D_{vn}$ (%)
0.01	2.02	0.052	0.00
0.02	4.07	0.052	0.00
0.04	6.05	0.051	1.92
0.06	8.17	0.05	3.85
0.08	10.21	0.05	3.85
0.1	12.84	0.049	5.77
0.25	15.29	0.047	9.62
0.5	18.85	0.045	13.46
0.75	21.74	0.025	51.92
1	23.88	0.011	78.85

increased at 0.5 mL/min. The results are shown in Table 1 and Figure 7, respectively.

It can be seen from the test results of No. 1 core that with the increase in displacement rate, the permeability shows a downward trend, which is due to the occurrence of particle migration and the blockage of pore channels by small particles, resulting in the decrease in permeability. Permeability decreases significantly when the flow rate is



(a)



(b)

**Figure 6:** Relationship between the parameters of No. 1 core and the displacement velocity: (a)  $D_{vn}$  vs displacement velocity. (b) Liquid permeability vs displacement velocity.



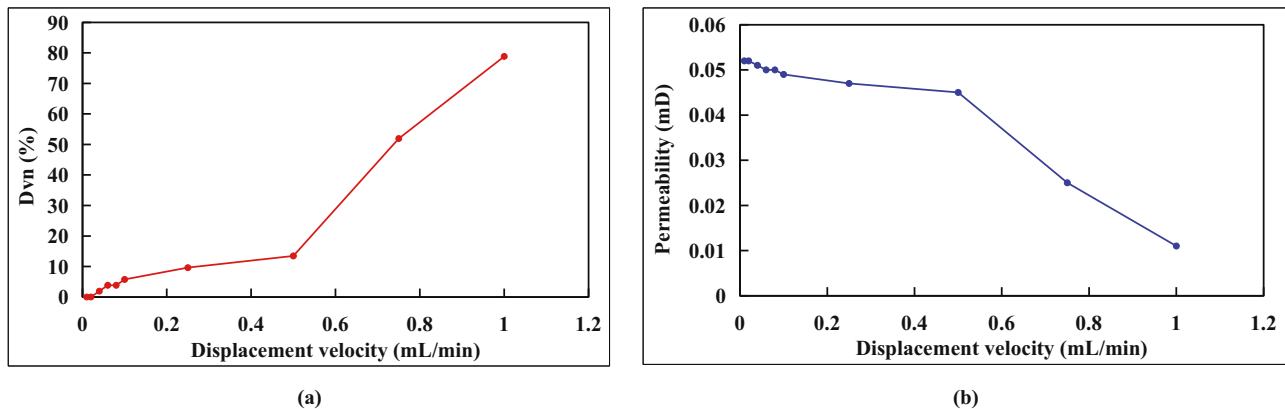


**Figure 7:** Relationship between the parameters of No. 2 core and the displacement velocity: (a)  $D_{vn}$  vs displacement velocity. (b) Liquid permeability vs displacement velocity.

greater than 0.04 mL/min, and therefore the displacement rate should be less than 0.04 mL/min in the possible core displacement experiment to exclude the influence of velocity sensitivity.

Based on the results of No. 2 core velocity sensitivity test, it can be seen that with the increase in displacement rate, the permeability shows a downward trend, and when the flow rate is greater than 0.5 mL/min, the permeability decreases significantly. Core No. 2 has higher permeability and thus higher critical velocity.

The comprehensive experimental results show that the content of cement and clay in M reservoir is relatively high. In the oil development process, because the water injection rate or the pressure relief of production wells are too fast, the particles are easier to migrate, which changes the pore structure characteristics of the reservoir, resulting in serious velocity-sensitivity damage to the reservoir near the wellbore as well as poorer permeability of the reservoir. Therefore, it is very important to study the type, content of clay minerals, and the formation sensitivity in M reservoir. It can be predicted that under the condition of long-term water injection, part of the seepage channels will increase, the permeability will also increase accordingly, and the micro-heterogeneity will show a certain decreasing trend. Whereas for the inferior formation of M reservoir with lower permeability, the permeability will be getting lower and lower due to the velocity sensitivity, which greatly increases the intrastratal and interlayer permeability difference. On the one hand, water channeling of injected water along the big pore causes serious water flooding of oil wells, on the other hand, due to the heterogeneity of reservoirs, the degree of water sweeping in poor reservoirs is weak, resulting in the enrichment of remaining oil. Therefore, in the process of water injection and oil

production in M reservoir, the injection and production rate should be controlled reasonably and seriously to reduce the damage of low permeability reservoir caused by velocity sensitivity.

## 5 Conclusion

The M reservoir in Karamay oil field is characterized by high clay mineral content, loose inter-particle cementation and strong velocity sensitivity. In the process of water flooding, the reservoir permeability decreases, which seriously affects the injection capacity of injection wells and the development effect of production wells. Two reservoir cores were selected to carry out velocity sensitivity experiments. The permeability of No. 1 core decreased obviously after the flow rate was greater than 0.04 mL/min. Permeability of No. 2 core is relatively high, when the flow rate is greater than 0.5 mL/min, the permeability decreased significantly. Based on the test results of No. 1 and No. 2 cores, it can be concluded that the injection rate of velocity sensitivity in M reservoir is around 0.04 and 0.5 mL/min. The study can provide a basis for the selection of displacement velocity in core experiments, and also provide a reference for the determination of reasonable injection-production velocity in actual production, so as to guide the oil field to further optimize the development plan and ensure the production.

**Funding information:** This work was supported by Scientific Research and Technology Development Project of PetroChina Company Limited (Grant No.: 2021DJ1103), Major Science and Technology Projects of PetroChina Company Limited (Grant No.: 2021ZZ01), Open Fund of State Key Laboratory of



Enhanced Oil Recovery, PetroChina Company Limited (Grant Nos.: 2022-KFKT-29 and RIPED-2022-JS-2156).

**Author contributions:** Conceptualization, Haishui Han, Qun Zhang and Weifeng Lv; methodology, Weifeng Lv, Lu Han, Zemin Ji and Hao Kang; formal analysis, Shanyan Zhang, Changhong Zhao and Hao Kang; investigation, Hao Kang; resources, Hao Kang, Linghui Sun and Rui Shen; writing—original draft preparation, Hao Kang and Haishui Han; writing—review and editing, Hao Kang and Haishui Han; supervision, Haishui Han, Qun Zhang, and Weifeng Lv; project administration, Haishui Han, Qun Zhang, and Weifeng Lv; funding acquisition, Qun Zhang and Weifeng Lv. All authors have read and agreed to the published version of the manuscript.

**Conflict of interest:** The authors declare that the research was conducted in the absence of any commercial or financial relationships that could be construed as a potential conflict of interest.

## References

- [1] Le K, Zhang L, Li Y. The impact of the Russia-Ukraine conflict on energy price volatility from the perspective of Internet's attention. *Prices Monthly*. 2022;(9):24–32.
- [2] Yu P. Research on the impact of the Russia-Ukraine conflict on China's energy trade and countermeasures. *Prices Mon*. 2022;(9):73–7.
- [3] Liu M. The influence of Russian-Ukrainian situation on energy market and countermeasure suggestions. *Pet Petrochem Today*. 2022;30(4):1–4, 10.
- [4] Liu Z, Yan Z, Hou Y. The impact and implication of Russia-Ukraine conflict on world energy development. *J Glob Energy Interconnect*. 2022;5(4):309–17.
- [5] Wang W, Li D. Research on international commodity price trend and China's countermeasures. *Prices Monthly*. 2022;(7):14–8.
- [6] Liu L. The backfire of financial sanctions on the US dollar standard. *J Northeast Norm Univ (Philos Soc Sci)*. 2022;5:107–11.
- [7] Li G, Lei Z, Dong W, Wang H, Zheng X, Tan J. Progress, challenges and prospects of unconventional oil and gas development of CNPC. *China Pet Explor*. 2022;27(1):1–11.
- [8] Wang Y. Characteristics of unconventional oil and gas plays and thoughts on resource management. *China Pet Explor*. 2022;27(3):20–6.
- [9] Huang C, Huo L, Wu C. Progress and prospect of CO<sub>2</sub> resource utilization technology based on unconventional oil and gas development. *Unconv Oil Gas*. 2022;9(1):1–9.
- [10] Li Y, Zhang D, Fan X, Zhang J, Yang R, Ye H. EOR of CO<sub>2</sub> flooding in low-permeability sandy conglomerate reservoirs. *Xinjiang Pet Geol*. 2022;43(1):59–65.
- [11] Jiang M. Analysis of oil production technology measures suitable for low permeability oilfield. *Total Corros Control*. 2022;36(6):77–8, 81.
- [12] Huang W, Wen R, Pang J, Sun Y, Yang W. Experiment on injection parameter optimization for air foam flooding in low-permeability heterogeneous reservoir. *Spec Oil Gas Reserv*. 2021;28(3):124–9.
- [13] Lu S, Wu X, Zhao Y, Xu T. Research on evaluation of velocity sensitivity to reservoirs of Nanpu Oilfield. *Drill Fluid Completion Fluid*. 2011;28(3):28–30.
- [14] Wang P, Ouyang C, Chen H, Chen X. Application of PCA and multiple nonlinear regression to rapid prediction of reservoir sensitivity. *Fault-Block Oil Gas Field*. 2018;25(2):232–5.
- [15] Sun H, Xu J, Yu Z, Wang D, Ma H, Ma T. Gas/liquid equivalence evaluation method for the sensitivity of coal reservoir to flow velocity. *Oil Drill Prod Technol*. 2019;41(4):509–15.
- [16] Ao K, Liu Y, Qin D. Speed sensitive effect on micro fracture rocks under different stress. *J Daqing Pet Inst*. 2010;34(6):64–7, 71.
- [17] Zhang F, Yue X, Pang H. Effect of pressure sensitivity on production rate in low permeability sandstone formation. *Oil Drill Prod Technol*. 2007;29(1):69–71.
- [18] Shi J, Gong W, Cao W, Xu Y. A Research into the Damage Mechanism of Velocity-Sensitivity in Sandstone of a Reservoir. *J Chengdu Univ Technol (Sci Technol Ed)*. 2003;30(5):501–4.
- [19] He Y, You Q, Zhong H, Yan J. Study and application of the formation damage of potential sensitivity fast predicting software in Daqing oil field. *Drill Fluid Completion Fluid*. 2002;19(1):32–5.
- [20] Bai Y, Wang Y. Effect of fluid viscosity on the sensitivity of reservoir rock flowing velocity. *J Jiangnan Pet Inst*. 2003;25(1):79–80.
- [21] Yang B, Zhou Z, Chen C. Discussion of acidizing radius of speed sensitivity injectors of Xinganling Group. *J Hebei Univ Eng (Nat Sci Ed)*. 2011;28(1):100–5.
- [22] Chen L, Wang W. Lower penetration reservoirs core speed sensitivity evacuation test. *Petrochem Ind Technol*. 2015;22(7):133–4.